IEC-96

Report of Subgroup 4 to the Sixth Meeting of the

NEANSC WORKING PARTY ON INTERNATIONAL EVALUATION COOPERATION

ORNL, USA, 4-6, May, 1994

Re-evaluation of ^{238}U Inelastic Scattering Cross Section for JENDL-3.2

Y. Kanda

Evaluation of ^{238}U Inelastic Scattering Cross Section

Toshihiko Kawano, Noboru Fujikawa, and Yukinori Kanda

Department of Energy Conversion Engineering,
Kyushu University

6-1, Kasuga-kouen, Kasuga-shi, Fukuoka 816, Japan

ABSTRACT : A new evaluation of ^{238}U inelastic scattering cross sections has been made. A coupled-channels model is adopted for calculation of direct inelastic scattering cross sections to the excited levels which belong to the vibrational bands of ^{238}U, as well as the ground state rotational band. The members of a certain vibrational band are coupled to the 0^+-2^+-4^+ triad of the ground state rotational band levels. A band coupling strength β is determined from the experimental inelastic scattering data below 3 MeV. Experimental double differential cross sections (DDX) are also taken into account in the β determination. The calculated level excitation cross sections and the calculated DDX reproduce consistently the experimental data.

1. Introduction

Reliable neutron inelastic scattering cross sections for ^{238}U are demanded for reactor design. However, determination of the $^{238}U(n,n')$ cross sections is difficult because of scattered experimental data, and too complicated nuclear structure to calculate with nuclear models, and there are considerable discrepancies among the evaluated nuclear data libraries.

Discrete levels of ^{238}U at low excitation energies are classified into a ground state rotational band and a quadrupole, an octupole vibrational bands. A coupled channels (CC) model calculation of the direct inelastic scattering cross sections to the ground state rotational band levels ($0^+, 2^+, 4^+, \ldots$) has been successfully applied to analyze the experimental data[1]. While the excitation cross sections of the vibrational band members are usually evaluated with a DWBA (Ref.2, for example). This method, however, may bring some uncertainties into the evaluation, because the DWBA calculations are normalized to the experimental data, and there is a discrepancy between the γ-ray and neutron detected measurements for these levels. Recently the CC model was also adopted for the vibrational states by University of Lowell group[3,4,5], and the excitation cross sections of the levels were calculated up to 3 MeV. We adopt the CC calculation for the evaluation of the vibrational states, and determine a band coupling strength β independent of the Lowell group. The β is determined from the experimental inelastic scattering data below 3 MeV. Experimental double differential cross sections (DDX) at

1.2, 2.03, 4.25, 6.1, and 14 MeV are also included in the β determination.

The evaluated nuclear data library JENDL-3.2 contains the result of the present evaluation.

2. Discrete Level Assignment

In order to evaluate the inelastic scattering cross sections for ^{238}U, a level scheme of this nucleus has to be decomposed into collective band families. Figure 1 is the decomposed band level scheme which was given according to assignment in Ref.3, and the excitation energies and J^{π} of the levels were corrected according to Ref.6. The excited levels with small J value are taken into account, since the inelastic scattering cross sections to these levels are expected to be large. There are some levels that cannot be classified into the collective band families. We take 1059.3(3^+), 1112.6(1^-), 1224.2(2^+), 1278.5(1^-), and 1285.8(5^-) levels into competition in the calculation of the compound process. Above 1290 keV, the excited levels are assumed to be overlapped.

3. Ground State Rotational Band

The evaluation of the inelastic scattering cross sections for 2^+ and 4^+ levels is conducted by the CC calculation with a deformed optical potential parameter set for ^{238}U employing the 0^+-2^+-4^+ level coupling scheme proposed by Bruyères-le-Châtel group[1]. Contribution of the compound process for these levels is significant in the energy range $E_{thresh.} \leq E_n \leq 3$ MeV. The cross sections are given by Engelbrecht-Weidenmüller transformation[7] which is an extension of the Hauser-Feshbach theory when strong absorption channels exist. The competition of a radiative capture channel is taken into account since the influence cannot be ignored near threshold energy of 44.91 keV(2^+) level. The calculation of the cross section of direct and compound process is carried out with ECIS88[8].

The calculated radiative capture cross section is somewhat different from the evaluation of JENDL-3. In addition, a fission channel must be taken into account. The compound inelastic scattering cross sections are normalized so as to conserve a compound formation cross section $\sigma_{CN}(= \sigma_R^{Opt.} - \sum \sigma_{DI}^{i\text{-th level}})$, when the capture and the fission cross sections in JENDL-3 are considered.

Comparisons of the calculated inelastic scattering cross sections for the 2^+, 4^+, and 6^+ levels with the experimental data[1,9,10,11,12,13] are shown in Fig. 2. The evaluated nuclear data libraries — JENDL-3, ENDF/B-VI, BROND-2, and CENDL-2 – are also depicted in this figure. The differences among the evaluated data seem to be small for the 2^+, 4^+ levels, and they are consistent with the experimental data. There is obvious difference among the evaluations of 6^+ level. However, only one measurement[11] with relatively large uncertainty is available and thus the discrepancy cannot be solved from the data.

4. Vibrational Bands

The direct inelastic scattering cross sections for the vibrational bands are also evaluated with the CC calculation. The members of a certain vibrational band are coupled to the 0^+-2^+-4^+ triad of the ground state rotational band levels. The coupling between the different vibrational bands is ignored since the strength of the coupling is expected to be weak.

The compound process contribution for the vibrational levels is calculated using the Hauser-Feshbach theory with width fluctuation correction by Moldauer[14]. The optical-statistical model code CoH[15] is used for the calculation of compound inelastic scattering cross sections with a spherical optical potential parameter by Madland and Young[16]. The compound inelastic scattering cross sections are also adjusted as described in the previous section.

The band coupling strength β for each vibrational bands is estimated on the basis of the experimental level excitation cross sections. The available data are, Smith[10], Vorotnikov, *et al.*[13], Olsen, *et al.*[17], Shao, *et al.*[18], and Kazjula, *et al.*[18]. Once the band coupling strength β is obtained, the direct inelastic scattering cross sections for all levels in the band can be calculated simultaneously. Then the β has to be determined so as to be consistent with the experimental data for the considering band. Because the compound inelastic scattering cross section is dominant below $E_n = 2$ MeV, it is difficult to determine the β in this energy region. Then the β is estimated in the energy range $2 \le E_n \le 3$.

The calculated cross sections for the octupole $K = 0^-$ band levels — 680.1 keV(1^-), 731.9 keV(3^-), and 826.7 keV(5^-) — are shown in Fig. 3. As seen in Fig. 3, the CC calculation results in lower values in the energy range $2 \le E_n \le 5$ MeV than the experimental data which was obtained with the γ-ray measurements[15]. It is difficult to reproduce consistently these γ-ray detected data for these levels with the CC calculation. Then the neutron detected measurements are adopted to determine the β.

Comparisons of the calculated inelastic scattering cross sections to 950.2 keV(2^-, Octupole $K = 1^-$ band), 967.3 keV(2^+, 2γ band), and 1037.3 keV(2^+, β band) levels with the experimental data and the other evaluations are shown in Fig. 4. The present evaluations well represent the neutron detected experimental data denoted with the symbol o.

Figure 5 displays the total inelastic scattering cross sections (heavy solid curve), the partial excitation cross sections for all levels (light curves), and continuum inelastic scattering cross sections (heavy dotted curve). The same picture for JENDL-3 and

JEF-2 is also shown in Fig. 5. The total inelastic scattering cross section in the present evaluation and that in JENDL-3 are almost the same except for the energy range 45 keV $\leq E_n \leq$ 400 keV. The present evaluation gives lower values than that in JENDL-3. The other obvious differences are the level excitation cross sections of above 680 keV levels. The cross sections in JENDL-3 (light solid curves in Fig. 5) are larger than the present evaluations in the energy range 3 $\sim$ 20 MeV. The magnitude of the continuum inelastic cross section is defined as the difference between the non-elastic cross section and the other partial cross sections that are inelastic scattering to the discrete levels, fission, capture, $(n,2n)$, and $(n,3n)$.

5. Double Differential Cross Section

The CC calculations are extrapolated up to 20 MeV, and a double differential cross section (DDX) is calculated and the comparison with the experimental data are made, in order to confirm an amount of the inelastic scattering cross sections. The DDX is calculated using PLDDX[20]. The fission cross sections, ν, and the energy spectra are taken from JENDL-3. The experimental DDX data were measured by Baba, *et al.*[21], at E_n = 1.2, 2.03, 4.25, 6.1, and 14 MeV. 4.25 and 6.1 MeV data are important since contribution of the vibrational band levels at the excitation energies ~1 MeV is separated from the elastic group (0^+-2^+-4^+) and the experimental level excitation cross sections at these energies are not accessible.

The comparisons of calculated DDX and the experimental data at 6.1 MeV and $\theta = 30°$ are shown in Fig. 6. Note that the elastic scattering cross section was not included in the DDX calculation. As seen in this figure the present evaluation which is based on the CC calculation gives reasonable agreement with the DDX data around $Q = -1$ MeV where the inelastic scattering cross sections to the vibrational levels are dominant.

6. Conclusion

The new evaluation of the ^{238}U inelastic scattering cross sections was done. The direct process for the vibrational states was evaluated with the coupled-channels model. The calculated double differential cross sections with the present evaluation agree with the experimental data.

REFERENCES

[1] G.Haouat, J.Lachkar, Ch.Lagrange, J.Jary, J.Sigaud, and Y.Patin, *Nucl. Sci. Eng.*, **81**, 491(1982).

[2] P.E.Hodgson and A.M.Kobos, *Nucl. Sci. Eng.*, **89**, 111(1985).

[3] D.W.Chan, J.J.Egan, A.Mittler, and E.Sheldon, *Phys. Rev.*, **C26**, 841(1982).

[4] E.Sheldon, L.E.Beghian, D.W.S.Chan, A.Chang, G.P.Couchell, J.J.Egan, G.Goswami, G.H.R.Kegel, S.Q.Li, A.Mittler, D.J.Pullen, W.A.Schier, J.Q.Shao, and A.Wang, *J.Phys. G : Nucl. Phys.*, **12**, 443(1986).

[5] E.Sheldon, A.Aliyar, L.E.Beghian, J.J.Egan, G.H.R.Kegel, A.Mittler, and E.D.Athur, *Proc. Int. Conf. on Nuclear Data for Science and Technology*, Jülich, Germany, p.989(1991).

[6] E.N.Shurskikov, *Nuclear Data Sheets*, **53**, 601(1988).

[7] P.A.Moldauer, *Phys. Rev.*, **12**, 744(1976).

[8] J.Raynal, program ECIS88, unpublished.

[9] L.E.Beghian, G.H.R.Kegel, T.V.Marcella, B.K.Barnes, G.P.Couchell, J.J.Egan, A.Mittler, D.J.Pullen, and W.A.Schier, *Nucl. Sci. Eng.*, **69**, 191(1979).

[10] A.B.Smith, *Nucl. Phys.*, **47**, 633(1963).

[11] P.Guenther, D.Havel, and A.Smith, ANL/NDM-16(1975).

[12] F.Y.Tsang and R.M.Brugger, *Nucl. Sci. Eng.*, **65**, 70(1978).

[13] P.E.Vorotnikov, V.A.Vukolov, E.A.Koltypin, Ju.D.Molchanov, G.A.Otroshchenko, and G.B.Jan'kov, *Proc. 4th All Union Conf. on Neutron Physics*, Kiev, CIS, vol.2, p.119(1977).

[14] P.A.Moldauer, *Nucl. Phys.*, **A344**, 185(1980).

[15] T.Kawano, program CoH, unpublished.

[16] D.G.Madland and P.G.Young, *Proc. Int. Conf. Neutron Physics and Nuclear Data for Reactors and Other Applied Purposes*, Harwell, UK, p.349(1978).

[17] D.K.Olsen, G.L.Morgan, and J.W.McConnell, *Proc. Int. Conf. on Nuclear Cross Sections for Technology*, Knoxville, USA, p.677(1979).

[18] J.Q.Shao, G.P.Couchell, J.J.Egan, G.H.R.Kegel, S.Q.Li, A.Mittler, D.J.Pullen, and W.A.Schier, *Nucl. Sci. Eng.*, **92**, 350(1986).

[19] B.G.Kazjula, E.M.Kozulin, L.A.Pobedonostsev, G.A.Tutin, Ju.A.Nemilov, L.N.Sysoeva, and A.A.Filatenkov, *Jadernye Konstanty, Obninsk reports*, **4/39**, 14(1980).

[20] S.Chiba, PLDDX, unpublished.

[21] M.Baba, H.Wakabayashi, N.Ito, K.Maeda, and N.Hirakawa, *Nucl. Sci. Technol.*, **27**, 601(1990).

Figure Captions

Fig.1 Decomposition of the collective band level scheme of ^{238}U

Fig.2 Comparisons of the calculated and the experimental inelastic scattering cross sections to the ground state rotational band levels.

Fig.3 Comparisons of the calculated and the experimental inelastic scattering cross sections to the octupole $K^{\pi} = 0^-$ band levels.

Fig.4 Comparison of the calculated and the experimental inelastic scattering cross sections to 950.2keV(2^-) (the octupole $K^{\pi} = 1^-$ band), 967.3keV(2^+) (the quadrupole 2γ band), and 1037.3keV(2^+) (the quadrupole β band) levels.

Fig.5 Total, partial, and continuum inelastic scattering cross sections.

Fig.6 Comparison of the calculated and the experimental DDX at E_n =6.1MeV and $\theta = 30°$.

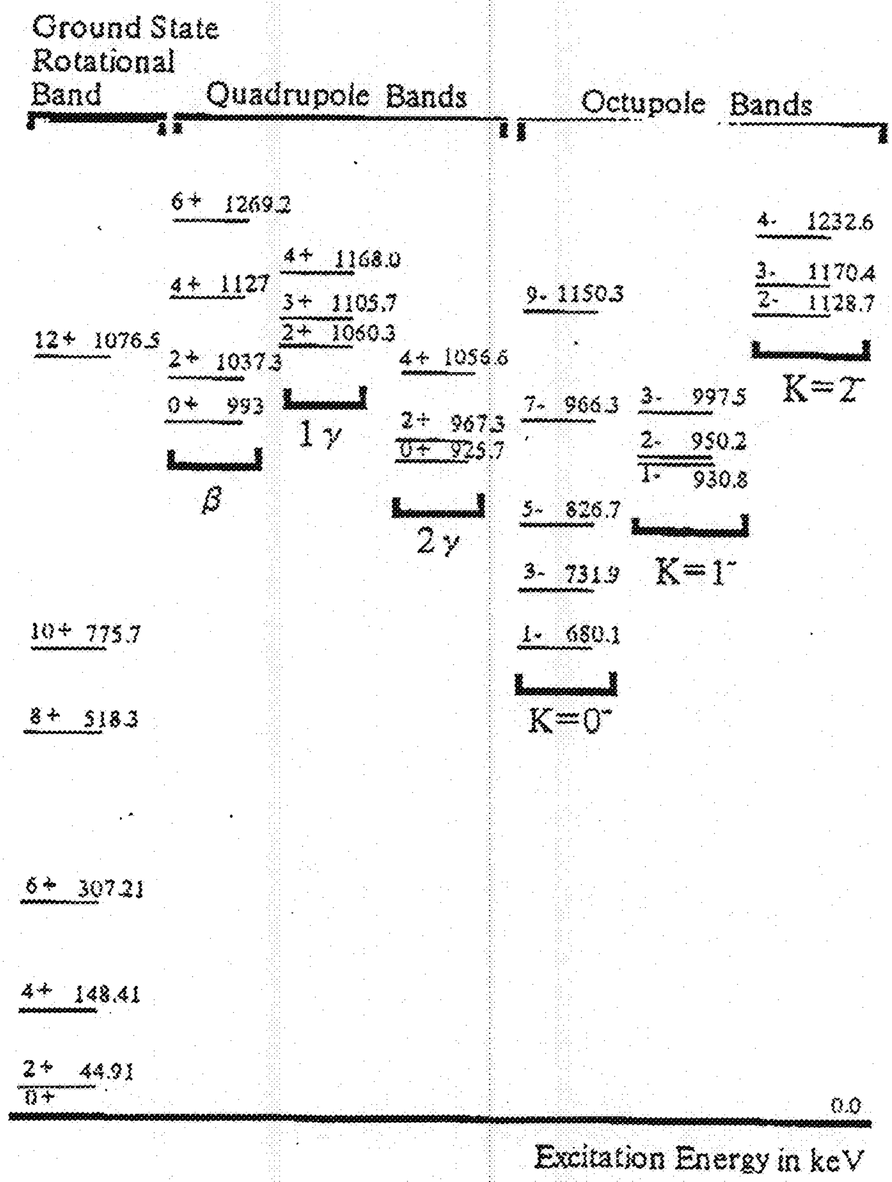
Ground State Rotational Band
Quadrupole Bands
Octupole Bands
6+ 1269.2
4+ 1127
2+ 1037.3
0+ 993
β
4+ 1168.0
3+ 1105.7
2+ 1060.3
1γ
4+ 1056.6
2+ 967.3
0+ 925.7
2γ
12+ 1076.5
10+ 775.7
8+ 518.3
6+ 307.21
4+ 148.41
2+ 44.91
0+
9- 1150.3
7- 966.3
5- 826.7
3- 731.9
1- 680.1
K=0⁻
3- 997.5
2- 950.2
1- 930.8
K=1⁻
4- 1232.6
3- 1170.4
2- 1128.7
K=2⁻
0.0
Excitation Energy in keV

Fig. 1

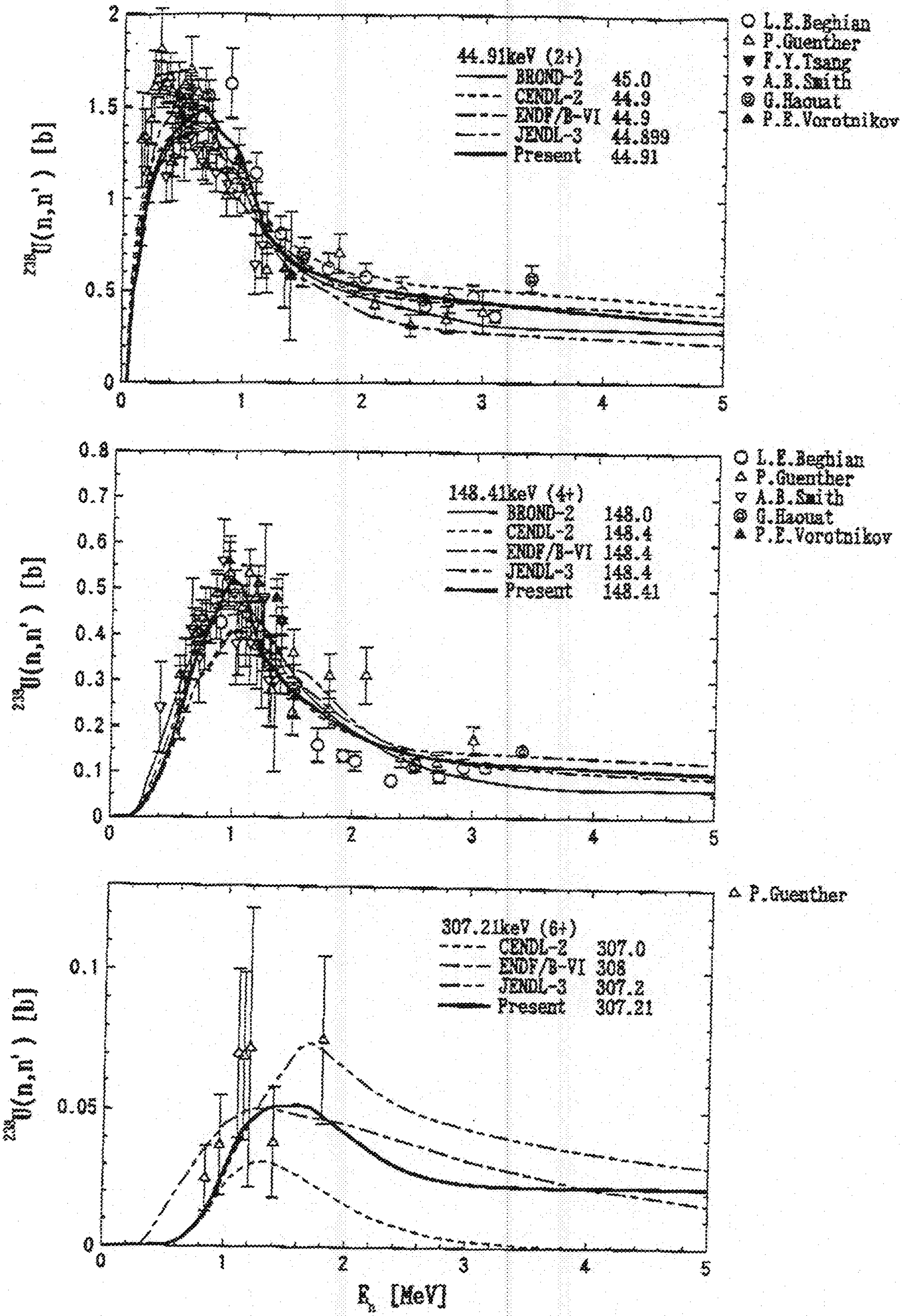

L.E.Beghian
P.Guenther
F.Y.Tsang
A.B.Smith
G.Haouat
P.E.Vorotnikov
44.91keV (2+)
BROND-2 45.0
CENDL-2 44.9
ENDF/B-VI 44.9
JENDL-3 44.899
Present 44.91
148.41keV (4+)
BROND-2 148.0
CENDL-2 148.4
ENDF/B-VI 148.4
JENDL-3 148.4
Present 148.41
307.21keV (6+)
CENDL-2 307.0
ENDF/B-VI 308
JENDL-3 307.2
Present 307.21
^{238}U(n,n') [b]
E_n [MeV]

fig. 2

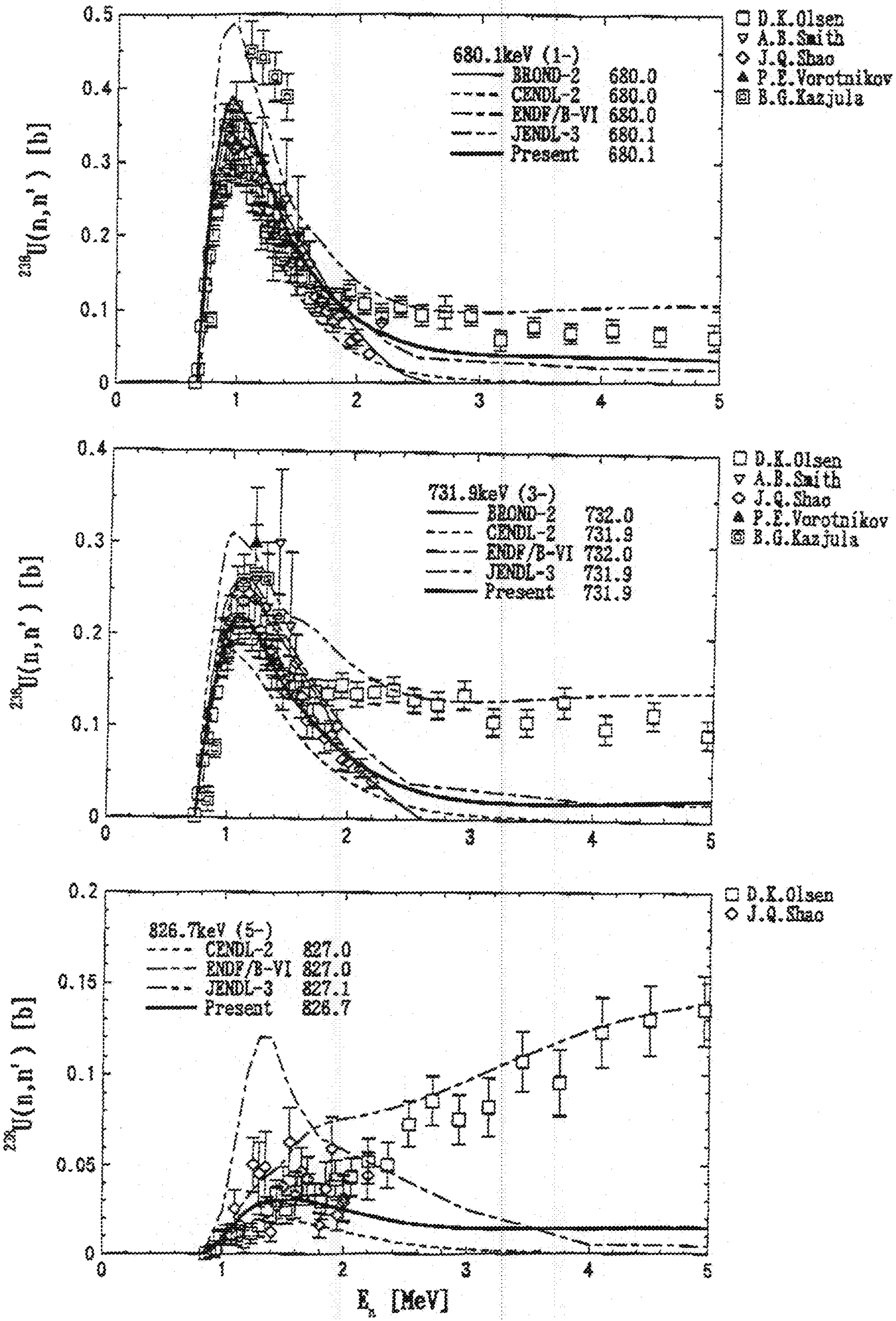

680.1keV (1-)
BROND-2 680.0
CENDL-2 680.0
ENDF/B-VI 680.0
JENDL-3 680.1
Present 680.1
D.K.Olsen
A.B.Smith
J.Q.Shao
P.E.Vorotnikov
B.G.Kazjula
^{238}U(n,n') [b]
731.9keV (3-)
BROND-2 732.0
CENDL-2 731.9
ENDF/B-VI 732.0
JENDL-3 731.9
Present 731.9
826.7keV (5-)
CENDL-2 827.0
ENDF/B-VI 827.0
JENDL-3 827.1
Present 826.7
E$_n$ [MeV]

Fig. 3

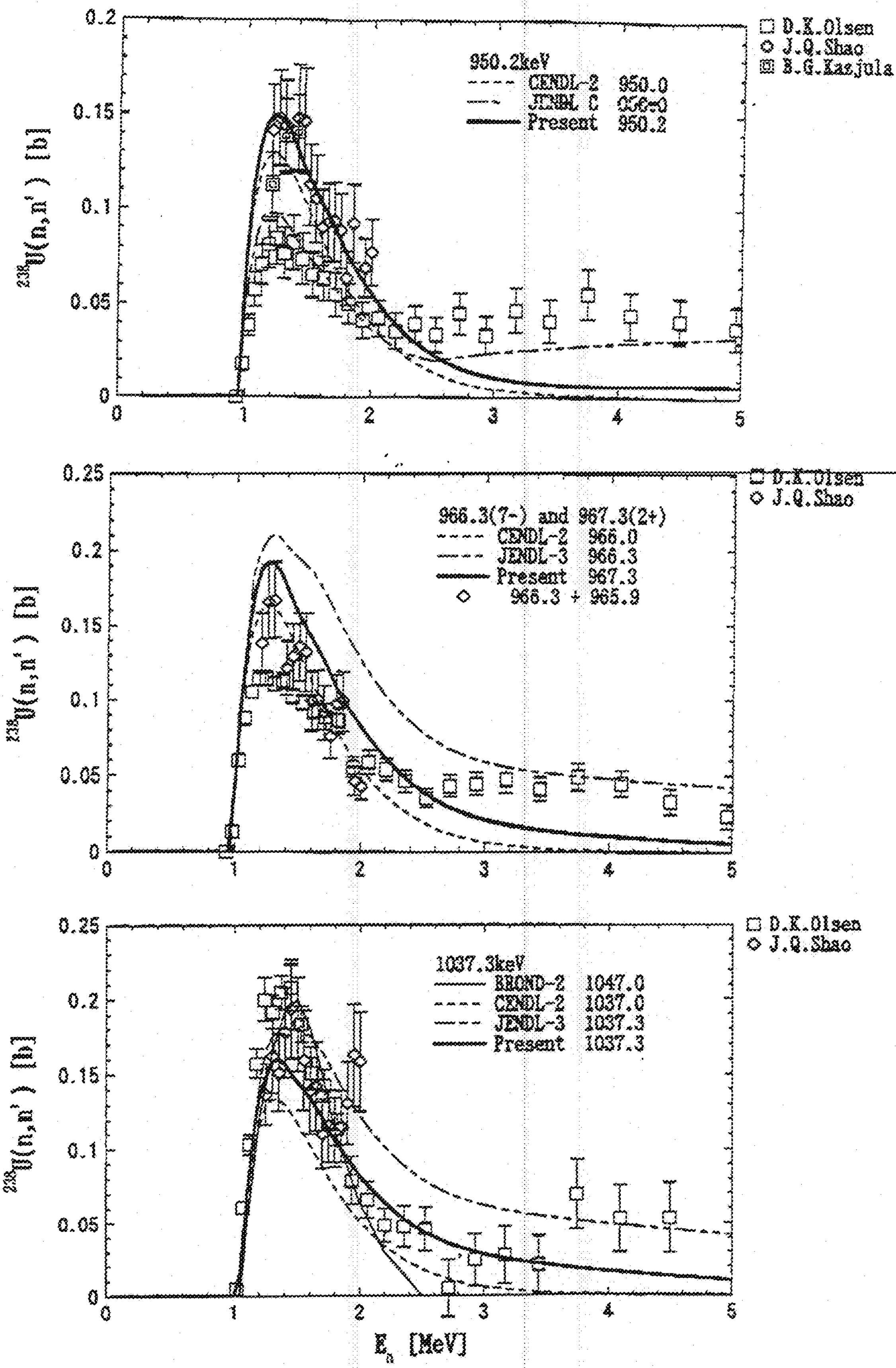
D.K.Olsen
J.Q.Shao
B.G.Kasjula
950.2keV
CENDL-2 950.0
Present 950.2
966.3(7-) and 967.3(2+)
CENDL-2 966.0
JENDL-3 966.3
Present 967.3
966.3 + 965.9
1037.3keV
BROND-2 1047.0
CENDL-2 1037.0
JENDL-3 1037.3
Present 1037.3
238U(n,n') [b]
En [MeV]

Fig 4

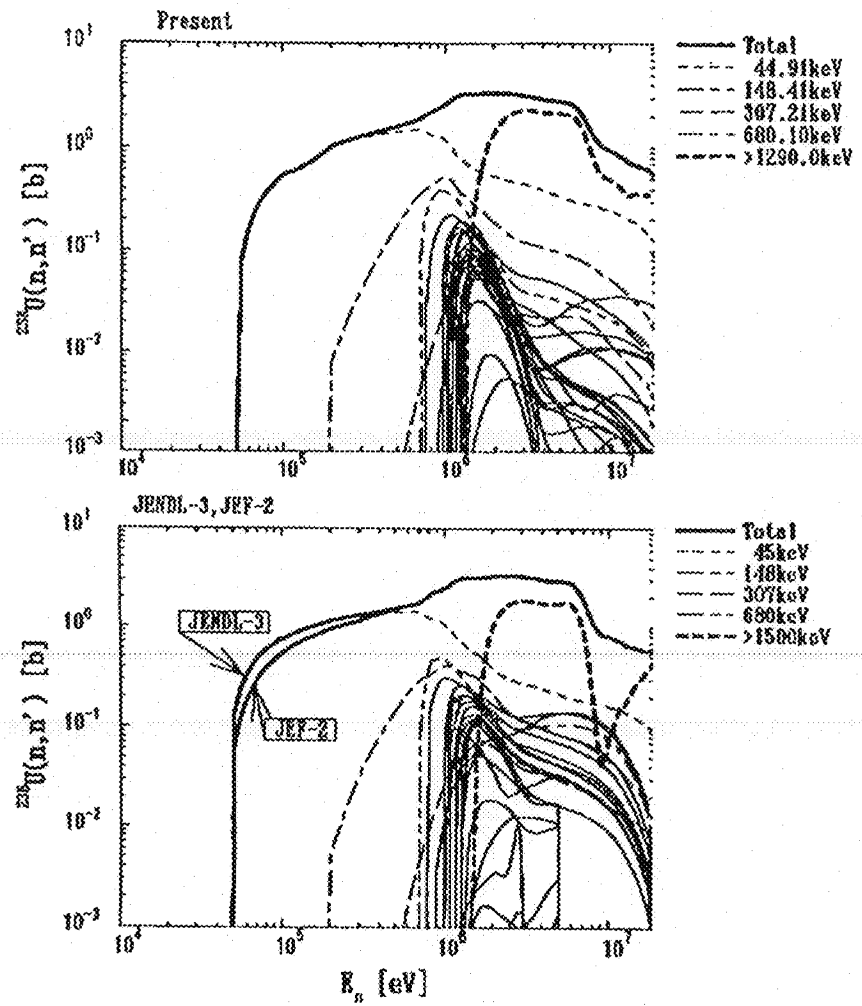
Present
Total
44.91keV
148.41keV
307.21keV
680.10keV
>1290.0keV
JENDL-3, JEF-2
Total
45keV
148keV
307keV
680keV
>1500keV
JENDL-3
JEF-2
E_n [eV]

Fig. 5

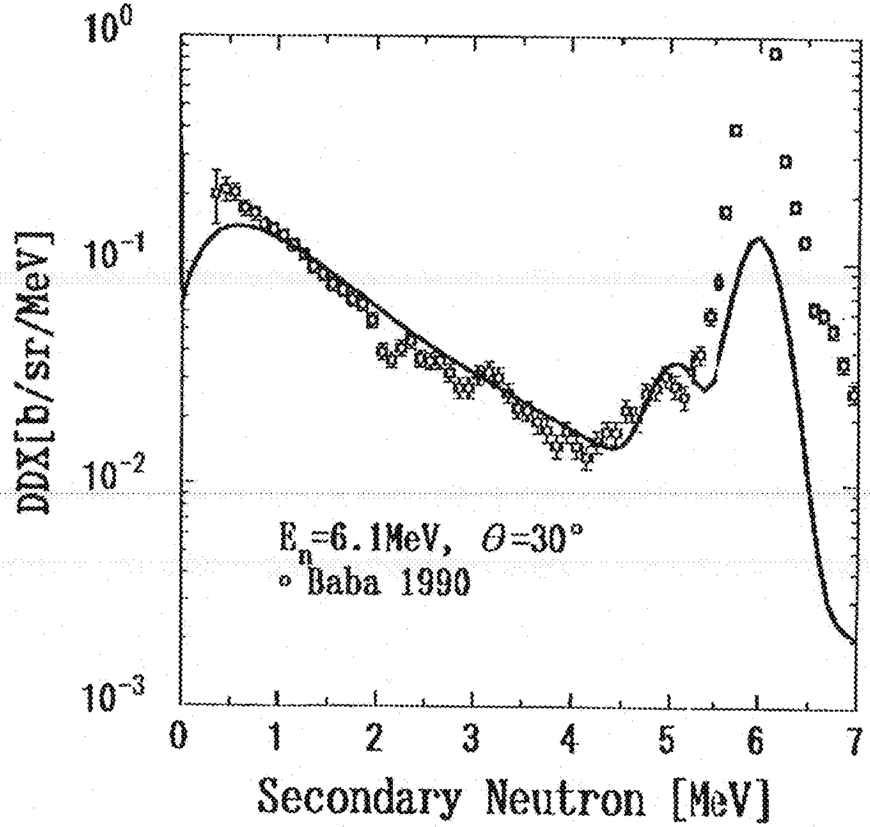
DDX[b/sr/MeV]
E_n=6.1MeV, θ=30°
∘ Baba 1990
Secondary Neutron [MeV]

Fig. 6